4-29-2013

Pre-breakdown evaluation of gas discharge mechanisms in microgaps

Abbas Semnani
Birck Nanotechnology Center, Purdue University, asemnani@purdue.edu

Ayyaswamy Venkattraman
Purdue University, venkatt@purdue.edu

Alina A. Alexeenko
Purdue University, alexeenk@purdue.edu

Dimitrios Peroulis
Birck Nanotechnology Center, Purdue University, dperouli@purdue.edu

AIP | Applied Physics Letters

Pre-breakdown evaluation of gas discharge mechanisms in microgaps

Abbas Semnani, Ayyaswamy Venkattraman, Alina A. Alexeenko, and Dimitrios Peroulis

Citation: Appl. Phys. Lett. **102**, 174102 (2013); doi: 10.1063/1.4803179
View online: http://dx.doi.org/10.1063/1.4803179
View Table of Contents: http://apl.aip.org/resource/1/APPLAB/v102/i17
Published by the AIP Publishing LLC.

Pre-breakdown evaluation of gas discharge mechanisms in microgaps

Abbas Semnani,[1,a)] Ayyaswamy Venkattraman,[2] Alina A. Alexeenko,[2] and Dimitrios Peroulis[1]
[1]*School of Electrical and Computer Engineering, Birck Nanotechnology Center, Purdue University, West Lafayette, Indiana 47907, USA*
[2]*School of Aeronautics and Astronautics, Purdue University, West Lafayette, Indiana 47907, USA*

(Received 14 February 2013; accepted 13 April 2013; published online 29 April 2013)

The individual contributions of various gas discharge mechanisms to total pre-breakdown current in microgaps are quantified numerically. The variation of contributions of field emission and secondary electron emission with increasing electric field shows contrasting behavior even for a given gap size. The total current near breakdown decreases rapidly with gap size indicating that microscale discharges operate in a high-current, low-voltage regime. This study provides the first such analysis of breakdown mechanisms and aids in the formulation of physics-based theories for microscale breakdown. © *2013 AIP Publishing LLC* [http://dx.doi.org/10.1063/1.4803179]

Strong electric fields in the order of tens of V/μm are encountered in micro/nano-scale gaps found in a wide variety of applications. Such strong fields may result in the formation of gas discharges leading to eventual breakdown which could degrade the performance or even result in device failure.[1,2] Understanding these phenomena is of critical importance not only for the plasma physics community but also for nano/microelectronics industries. Gas discharges are created due to the generation and transport of charged species as a result of three key mechanisms including electron-impact ionization (EII), secondary electron emission (SEE), and field emission (FE). When the generation rate of charged species exceeds that of losses, the rapid increase in the number of particles leads to gas breakdown.[3–5]

Both direct current (DC) and radio frequency (RF) discharges have been reported[6–12] with DC gas breakdown for relatively large microgaps ($>7\,\mu$m) well-studied especially at atmospheric pressure.[6,13–15] EII and SEE are the two main mechanisms of breakdown for these gaps and results in the Townsend avalanche breakdown leading to the Paschen curve.[3–5] However, experiments for smaller gaps have observed significant deviations from the Paschen curve.[16–18] It is now well established that FE, first theorized by Fowler and Nordheim,[19] is responsible for this deviation.[11,20,21] By including the effects of FE, the modified Paschen curve which merges micro and macroscale breakdown has been proposed.[14,15,22–24]

Gas discharge problems have been studied analytically,[13,14,22] semi-analytically,[20,25,26] numerically,[11,15,24] and experimentally[10,18,27,28] in DC, RF, and combined regimes.[26,28] The main goal of most of the previous studies was to predict the breakdown voltage for a given configuration.[6,14,23] More recently, other parameters such as discharge structure, discharge current, and particle densities were also investigated.[8,18,20,24,25]

Although different types of evaluation of discharge mechanisms have been reported,[11,20,21,24] a systematic characterization of the pre-breakdown mode for various operating conditions has not been presented. In particular, the main goal of this study is to use particle-in-cell with Monte Carlo collisions (PIC/MCC) simulations to quantify the contributions of EII, SEE, and FE mechanisms for DC breakdown in atmospheric pressure microgaps for several operating conditions near breakdown. These results provide a better understanding of the pre-breakdown characteristics of the discharge phenomena in order to both enhance the theoretical models and evaluate failure-free operating regimes in micro and nanoscale gaps.

EII is often referred to as an α-process where α is the ionization coefficient.[4] An empirical formula that describes the variation of α as a function of applied voltage V, electrode gap d, and gas pressure p is given by[4]

$$\alpha = Ape^{-Bpd/V}, \tag{1}$$

where A and B are gas-dependent constants. SEE from the cathode is another important discharge mechanism which is quantified by the SEE coefficient (γ_{se}) that depends on both the cathode material and the gas.[4] If we consider only EII and SEE, the traditional Paschen curve is obtained with the breakdown voltage given by[4]

$$V_b = \frac{Bpd}{\ln(pd) + \ln\left[\frac{A}{\ln(1/\gamma_{se}+1)}\right]}. \tag{2}$$

As mentioned earlier, the Paschen curve does not describe the breakdown process in microgaps where FE due to quantum tunneling of electrons plays a significant role. The FE current density is described by the Fowler-Nordheim (F-N) equation as follows:[19]

$$j_{FN} = \frac{A_{FN}\beta^2 E^2}{\varphi t^2(y)} \exp\left[-\frac{B_{FN}\varphi^{3/2} v(y)}{\beta E}\right], \tag{3}$$

where E is the electric field, φ is the work function of the cathode, β is the field enhancement factor, and A_{FN} and B_{FN} are the F-N constants.[29] β is a strong function of surface roughness, and its value has been reported in the range of 1.5–115 in various experiments for atomically rough surfaces.[30] The

[a)]Electronic mail: asemnani@purdue.edu

barrier shape function $v(y) \approx 0.95 - y^2$ and $t^2(y) \approx 1.1$ with $y \approx 3.79 \times 10^{-4}\sqrt{\beta E}/\varphi$ were included later.[31]

An approximate expression for V_b that considers only FE is given by[23]

$$V_b = \frac{d(D + Bp)}{\ln(KApd)}, \tag{4}$$

where K is a fitting parameter and D is defined as[16]

$$D = (6.85 \times 10^9)\frac{\varphi^{3/2}}{\beta}. \tag{5}$$

The modified Paschen curve that bridges pure FE driven breakdown with the traditional Paschen curve has been formulated[14] using the modified breakdown condition given by

$$(\gamma_{se} + Ke^{-Dd/V_b})\left[e^{Apd\ exp(-Bpd/V_b)} - 1\right] = 1, \tag{6}$$

where all three driving mechanisms—EII, SEE, and FE—have been included. The above equation does not have closed form solutions for V_b and should be solved numerically and has been shown to explain various experimental data for microscale breakdown.[14]

The geometrical configuration used in this study is shown in Fig. 1(a). It is assumed that the electrode plates are sufficiently large in comparison with the gap size to consider the problem in its simplified one-dimensional form.

In this study, PIC/MCC simulations[32–34] of gaps in the range of $0.5 - 10$ μm are considered including gaps in pure FE driven, transition, and macroscale regimes of the modified Paschen curve. Argon gas at room temperature of 300 K (0.026 eV) is the background gas. The electrodes are taken to be nickel with φ equal to 5.15 eV. β is equal to 55 which is a typical value reported in experiments performed using microstructures.[18] In the PIC/MCC simulations, the electronic excitation of argon is included, but the excited species are not tracked since it is assumed that their lifetimes are very short and do not contribute significantly to the breakdown process.

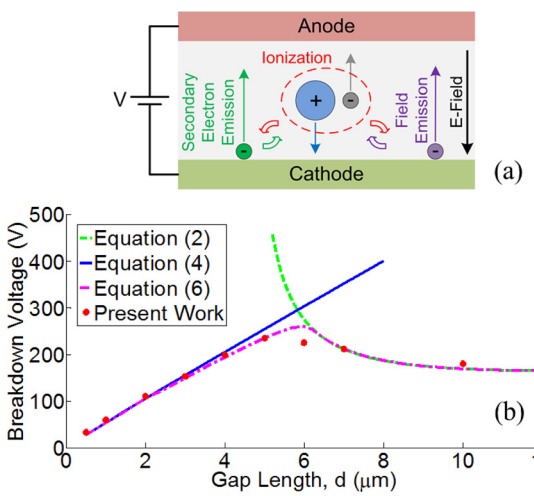

FIG. 1. (a) Geometrical configuration of the problem with interplay of discharge mechanisms and (b) comparison of breakdown voltage curve obtained in the current work with various models in literature.

Three sets of simulations were performed for this study and are briefly described below.

1. The gas pressure and γ_{se} are assumed to be zero leading to neither EII nor SEE. Therefore, the steady-state current in the first case is solely due to FE at the nominal electric field.
2. Gas pressure is considered equal to 1 atm with $\gamma_{se} = 0$ which leads to EII in the gas phase in addition to the FE. By comparing the discharge currents from the first two sets, the contribution of EII to the total current is obtained.
3. We retain the same conditions as the second set except that $\gamma_{se} = 0.05$ which is a reasonable value based on an empirical equation.[4] Here, we have the interplay of all mechanisms of gas breakdown. As a result, a comparison of the steady-state currents in the second and the third sets can be used to extract the contribution of SEE to the total discharge current.

Here, it is worth describing the interplay of the three mechanisms in more detail. The presence of a net positive charge modifies the electric field distribution in the gap slightly and its effect on FE which strongly depends on E is included in this study. The effect of ion-enhanced FE is included in the contribution of EII estimated using the above methods. Since this component of the FE current is a direct consequence of ionization and will be zero if no ions are produced, we consider it as a component of the EII current. Similarly, when the contribution of SEE is studied, it also includes additional ionization related to the electrons which are produced by SEE and ion-enhancement due to the ions produced by these electrons. It should be mentioned that the γ_{se} is assumed to be constant which is a good assumption due to the small change in E and the weak dependence of γ_{se} on that.

For investigating the effect of applied field (E_{app}), we consider four different values between about $0.75E_b$ and E_b where E_b is the breakdown field. By the applied field we mean the nominal external field while the actual field inside the gap is modified slightly as mentioned above. We used a trial-and-error method to find E_b as the applied field at which the number of computational particles diverged. For verification of our simulations, we compared our results with existing models, which have been experimentally validated, as shown in Fig. 1(b), and it can be observed that the agreement for E_b is very good.

Fig. 2 shows the contributions of FE, EII, and SEE to the total pre-breakdown current as a function of gap size and E_{app}. It is seen that FE is the dominant mechanism in very small gaps (<1 μm). However, its contribution is greatly reduced as the gap size is increased and becomes less than 5% for the 5 μm gap. This trend can be explained by considering the E_b values shown in Table I in which E_b decreases as the gap size increases.

In very small gaps, the FE current is quite high, but the ionization probability is low resulting in the production of very few ions. On the other hand, for large gaps, although the ionization probability is much higher, the number of electrons due to FE is small. Therefore, we expect the gas-phase ionization to have net maximum contribution in moderate-sized gaps. As seen in Fig. 2(b), it has a maximum

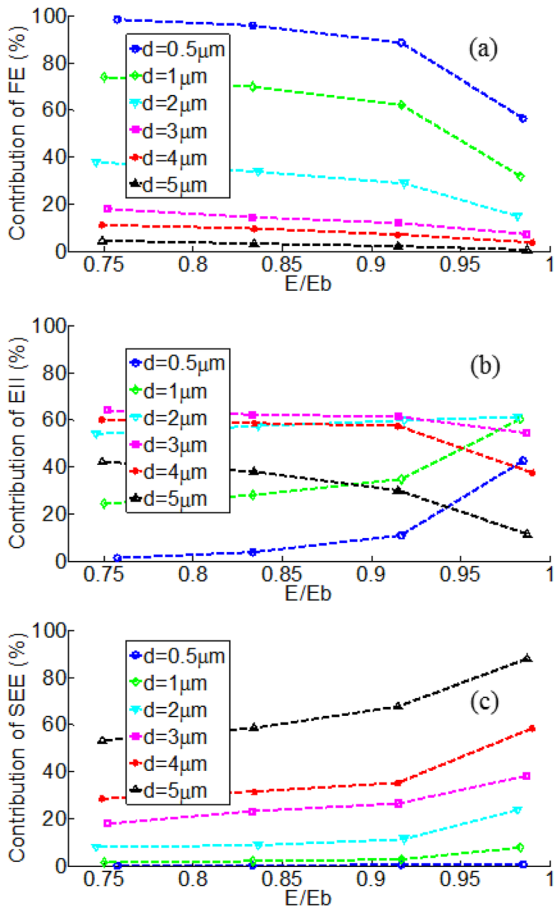

FIG. 2. Contribution of (a) field emission, (b) electron-impact ionization, and (c) SEE to total discharge current for various gap sizes and applied electric fields.

value of about 60% of total discharge current for the 3 μm gap.

When the effect of varying the applied field is considered, it is observed that in spite of the absolute value of FE current increasing with increasing E_{app} (Table I), its contribution to the total current decreases. For example, the FE current contributes almost 100% of the discharge current in 0.5 μm gap at an applied voltage of $0.75V_b$. However, it decreases to about 57% when the applied voltage approaches V_b. This is due to the higher rate of increase of EII and consequently SEE currents when the applied field is increased. It is interesting that, for a given gap size, the contribution of SEE increases monotonically with increase in both gap size and applied voltage. For the $\gamma_{se} = 0.05$ considered, SEE is the sole breakdown mechanism for gaps larger than about 5 μm.

Fig. 3 presents the absolute values of total discharge current densities as well as the contribution of electrons and ions to the total. It is observed that the contribution of electrons to the total current decreases as the gap size is increased, while the contrary is true for ions. Specifically, about 90% of the current is carried by electrons in the 0.5 μm gap, while about 80% of current is due to ions in the 5 μm gap. This is directly related to the increase in ion production as the gap size increases. Also, for a given gap size, increasing the applied voltage slightly decreases the electron and increases the ion contribution. It is also observed that the total discharge current significantly decreases while the gap size is increased. As an example, the discharge current in the 0.5 μm gap is about four orders of magnitude larger than the current in the 5 μm gap at an applied voltage of $0.75V_b$. This is a direct consequence of a lower breakdown field and hence a lower FE

TABLE I. Breakdown and applied voltages as well as absolute values of different parts of discharge current densities.

Gap (μm)	E_b (V/μm)	E_{app} (V/μm)	J_{FE} (A/m^2)	J_{EII} (A/m^2)	J_{SEE} (A/m^2)	J_e (A/m^2)	J_i (A/m^2)
0.5	66	65	6.13×10^5	4.63×10^5	7.57×10^3	9.72×10^5	1.12×10^5
		60.5	1.1×10^5	1.36×10^4	530	1.13×10^5	1.11×10^4
		55	9.21×10^3	370	35.1	8.92×10^3	697
		50	616	8.7	1.46	592	35
1	60	59	5.8×10^4	1.1×10^5	1.43×10^4	1.26×10^5	5.68×10^4
		55	9.21×10^3	5.15×10^3	424.4	1.04×10^4	4.41×10^3
		50	616.7	247.3	18.4	637	246
		45	23.1	7.67	0.5	23	8
2	55	54	5.6×10^3	2.3×10^4	9.02×10^3	1.69×10^4	2.1×10^4
		50.5	827.7	1.72×10^3	327.6	1.32×10^3	1.55×10^3
		46	47.3	80.4	12.3	67	73
		41	0.96	1.38	0.21	1.29	1.26
3	51	50.3	759.5	6.65×10^3	3.97×10^3	3.12×10^3	7.25×10^3
		46.7	73.9	379.1	163.4	190	427
		42.5	3.34	14.36	5.34	7.7	15.4
		38.3	0.082	0.29	0.081	0.17	0.29
4	49.75	49.25	411.6	4.02×10^3	6.24×10^3	2.68×10^3	7.99×10^3
		45.5	30.18	241.1	147.9	109	311
		41.5	1.475	8.95	4.81	4.2	11.1
		37.25	0.026	0.138	0.066	0.07	0.16
5	47	46.4	63.69	1.04×10^3	8.03×10^3	1.67×10^3	7.46×10^3
		43	5.05	69.06	155.4	44.2	185.3
		39.2	0.18	2.06	3.17	1.09	4.32
		35.2	0.003	0.026	0.033	0.013	0.049

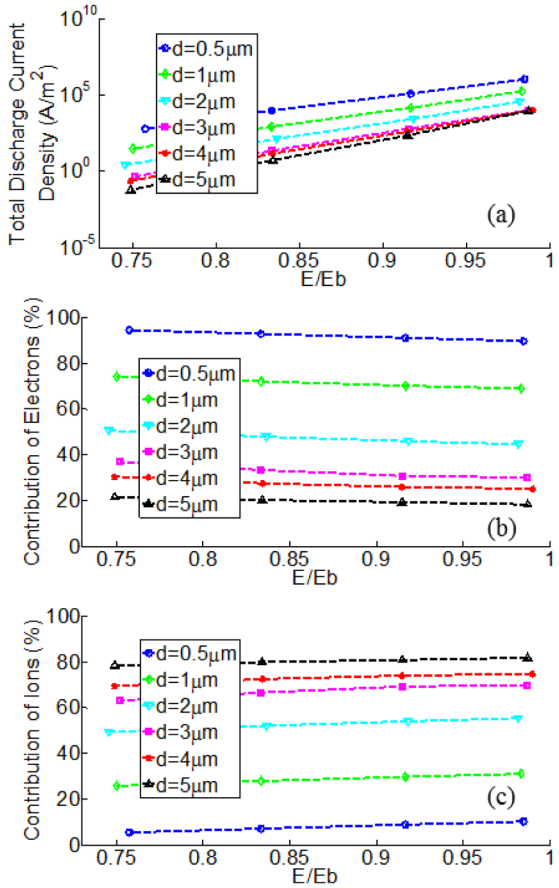

FIG. 3. (a) Absolute value of total discharge current densities as well as the contribution of (b) electrons and (c) ions for various gap sizes and applied electric fields.

current for larger gaps as shown in Table I. The analysis was also performed for $6-10\,\mu$m gaps though not explicitly shown here. For the chosen values of β, the contribution of FE which is the primary source of electrons is negligible in these gaps, and the steady-state discharge current is very small resembling classical low-current dark discharges.[4]

In summary, the pre-breakdown contribution of discharge mechanisms including EII, SEE, and FE in the total discharge current in microgaps has been investigated. This was accomplished using the PIC/MCC method for one-dimensional atmospheric pressure gaps. The dependence of the contributions on key parameters such as gap size and applied electric field were presented. It was concluded that FE contributes greater than 50% of the total current in gaps smaller than 1 μm. On the other hand, large percentage contributions were observed for SEE for larger gap sizes. For a given gap size, increasing the applied voltage leads to a decrease in the contribution of FE and an increase in the contribution of SEE to the total current. Most of the discharge current is due to electrons for very small gaps. However, the contribution of ions becomes dominant in larger gaps as the ionization probabilities increase leading to the production of more ions. It has also been shown that the total current density rapidly decreases with increasing gap size indicating that microdischarges typically operate in the high-current regime. The numerical results presented here are critical in understanding discharge problem and will complement the formulation of physics-based breakdown theories for micro-scale gas breakdown.

This paper is based upon work supported by the National Science Foundation under Grant No. 1202095.

[1]C. H. Chen, J. A. Yeh, and P. J. Wang, J. Micromech. Microeng. **16**(7), 1366 (2006).
[2]B. N. Sismanoglu and J. Amorim, Eur. Phys. J. Appl. Phys. **41**(2), 165 (2008).
[3]M. A. Lieberman and A. J. Lichtenberg, *Principles of Plasma Discharges and Materials Processing* (Wiley-Interscience Publication, 2005).
[4]Y. P. Raizer, V. I. Kisin, and J. E. Allen, *Gas Discharge Physics* (Springer-Verlag, Berlin, 1991).
[5]A. Fridman and L. A. Kennedy, *Plasma Physics and Engineering* (CRC, 2004).
[6]M. Klas, Š. Matejčík, B. Radjenović, and M. Radmilović-Radjenović, Phys. Scr. **83**(4), 045503 (2011).
[7]M. Savic, M. Radmilovic-Radjenovic, M. Suvakov, S. Marjanovic, D. Maric, and Z. L. Petrovic, IEEE Trans. Plasma Sci. **39**(11), 2556–2557 (2011).
[8]F. Iza, J. K. Lee, and M. G. Kong, Phys. Rev. Lett. **99**(7), 075004 (2007).
[9]H. B. Smith, C. Charles, and R. W. Boswell, Phys. Plasmas **10**, 875 (2003).
[10]J. L. Walsh, Y. T. Zhang, F. Iza, and M. G. Kong, Appl. Phys. Lett. **93**(22), 221505 (2008).
[11]A. Semnani, A. Venkattraman, A. Alexeenko, and D. Peroulis, in IEEE International Conference on Electromagnetics in Advanced Applications (ICEAA), 2012, pp. 803–806.
[12]V. Lisovskiy, J. P. Booth, K. Landry, D. Douai, V. Cassagne, and V. Yegorenkov, EPL **80**(2), 25001 (2007).
[13]M. Radmilović-Radjenović and B. Radjenović, Plasma Sources Sci. Technol. **17**(2), 024005 (2008).
[14]D. B. Go and D. A. Pohlman, J. Appl. Phys. **107**(10), 103303 (2010).
[15]M. Radmilović-Radjenović, J. K. Lee, F. Iza, and G. Y. Park, J. Phys. D: Appl. Phys. **38**(6), 950 (2005).
[16]W. S. Boyle and P. Kisliuk, Phys. Rev. **97**(2), 255 (1955).
[17]F. Iza, G. J. Kim, S. M. Lee, J. K. Lee, J. L. Walsh, Y. T. Zhang, and M. G. Kong, Plasma Processes Polym. **5**(4), 322–344 (2008).
[18]A. Venkattraman, A. Garg, D. Peroulis, and A. A. Alexeenko, Appl. Phys. Lett. **100**(8), 083503 (2012).
[19]R. H. Fowler and L. W. Nordheim, Proc. R. Soc. London, Ser. A **119**(781), 173–181 (1928).
[20]P. Rumbach and D. B. Go, J. Appl. Phys. **112**(10), 103302 (2012).
[21]M. Radmilović-Radjenović, Š. Matejčik, M. Klas, and B. Radjenović, J. Phys. D: Appl. Phys. **46**(1), 015302 (2013).
[22]R. Tirumala and D. B. Go, Appl. Phys. Lett. **97**(15), 151502 (2010).
[23]M. Radmilović-Radjenović and B. Radjenović, EPL **83**(2), 25001 (2008).
[24]Y. Li, R. Tirumala, P. Rumbach, and D. B. Go, IEEE Trans. Plasma Sci. **41**(1), 24–35 (2013).
[25]A. Venkattraman and A. A. Alexeenko, Phys. Plasmas **19**(12), 123515 (2012).
[26]M. Radmilović-Radjenović and B. Radjenović, Plasma Sources Sci. Technol. **15**(1), 1 (2006).
[27]A. Garg, V. Ayyaswamy, A. Kovacs, A. Alexeenko, and D. Peroulis, in IEEE 24th International Conference on Micro Electro Mechanical Systems (MEMS), 2011, pp. 412–415.
[28]V. A. Lisovskiy, N. D. Kharchenko, and V. D. Yegorenkov, J. Phys. D: Appl. Phys. **43**(42), 425202 (2010).
[29]R. Good and E. Müller, *Field Emission, Encyclopedia of Physics* (Springer-Verlag, 1957).
[30]T. E. Stern, B. S. Gossling, and R. H. Fowler, "Further studies in the emission of electrons from cold metals," Proc. R. Soc. London, Ser. A **124**(795), 699–723 (1929).
[31]R. E. Burgess, H. Kroemer, and J. M. Houston, Phys. Rev. **90**, 515 (1953).
[32]C. K. Birdsall, IEEE Trans. Plasma Sci. **19**(2), 65–85 (1991).
[33]J. P. Verboncoeur, M. V. Alves, V. Vahedi, and C. K. Birdsall, J. Comput. Phys. **104**(2), 321–328 (1993).
[34]V. Vahedi, G. DiPeso, C. K. Birdsall, M. A. Lieberman, and T. D. Rognlien, Plasma Sources Sci. Technol. **2**(4), 261 (1993).